



Research article

CENPA and *BRCA1* are potential biomarkers associated with immune infiltration in heart failure and pan-cancer

Jian Wang^{a,b}, Lin Cai^{a,b}, Gang Huang^{a,b}, Chunbin Wang^{a,b}, Zhen Zhang^{a,b,c}, Junbo Xu^{a,b,c,*}

^a Department of Cardiology, The Affiliated Hospital of Southwest Jiaotong University, 82 Qinglong Street, Chengdu, 610014, China

^b Department of Cardiology, The Third People's Hospital of Chengdu, 82 Qinglong Street, Chengdu, 610014, China

^c Chengdu Institute of Cardiovascular Disease, 82 Qinglong Street, Chengdu, 610014, China

A B S T R A C T

Heart failure (HF) and cancer are the two leading causes of death worldwide and affect one another in a bidirectional way. We aimed to identify hub therapeutic genes as potential biomarkers for the identification and treatment of HF and cancer. Gene expression data of heart samples from patients with ischemic HF (IHF) and healthy controls were retrieved from the GSE42955 and GSE57338 databases. Difference analysis and weighted gene co-expression network analysis (WGCNA) were used to identify key modules associated with IHF. The overlapping genes were subjected to gene and protein enrichment analyses to construct a protein-protein interaction (PPI) network, which was screened for hub genes among the overlapping genes. A total of eight hub genes were subjected to correlation, immune cell infiltration, and ROC analyses. Then we analyzed the roles of two significant genes in 33 tumor types to explore their potential as common targets in HF and cancer. A total of 85 genes were identified by WGCNA and differentially expressed gene (DEG) analyses. *BRCA1*, *MED17*, *CENPA*, *RXRA*, *RXRβ*, *SMARCA2*, *CDCA2*, and *PMS2* were identified as the hub genes with IHF. Finally, *CENPA* and *BRCA1* were identified as potential common targets for IHF and cancer. These findings provide new perspectives for expanding our understanding of the etiology and underlying mechanisms of HF and cancer.

1. Introduction

Heart failure (HF) and cancer are global health issues associated with high morbidity and mortality [1,2]. Several epidemiological studies have demonstrated an association of HF with subsequently increased risk of cancer [3–6]. In addition to risk factors including hypertension, diabetes, obesity, smoking, HF and cancer also share common pathophysiological mechanisms including inflammation, oxidative stress, neuro-hormonal activation and a dysfunctional immune system [7–10]. Previous studies showed chemotherapy-related cardiotoxicity or cancer itself might lead to HF [11–13]. Conversely, HF could stimulate and promote cancer progression and metastasis via cardiac excreted factors [14,15]. HF and cancer affect one another in this bidirectional way. Herein, we aimed to investigate the common targets and interactions of HF and cancer by transcriptomic analyses.

In this study, we obtained gene expression data from the Gene Expression Omnibus (GEO) database and identified differentially expressed genes (DEGs) between HF and normal samples using the GSE42955 and GSE57338 databases. Moreover, weighted gene co-expression network analysis (WGCNA) was performed on the GSE57338 dataset to screen key co-expression modules to assist in candidate hub gene selection. The CytoHubba algorithm was used to screen hub genes. A total of eight hub genes were subjected to correlation, immune cell infiltration, and ROC analyses. We further analyzed the roles of two significant genes *CENPA* and *BRCA1* in 33

* Corresponding author. Department of Cardiology, The Affiliated Hospital of Southwest Jiaotong University, 82 Qinglong Street, Chengdu, 610014, China.

E-mail address: xujunbo0723@126.com (J. Xu).

<https://doi.org/10.1016/j.heliyon.2024.e28786>

Received 18 August 2023; Received in revised form 24 March 2024; Accepted 25 March 2024

Available online 27 March 2024

2405-8440/© 2024 The Authors. Published by Elsevier Ltd. This is an open access article under the CC BY-NC license (<http://creativecommons.org/licenses/by-nc/4.0/>).

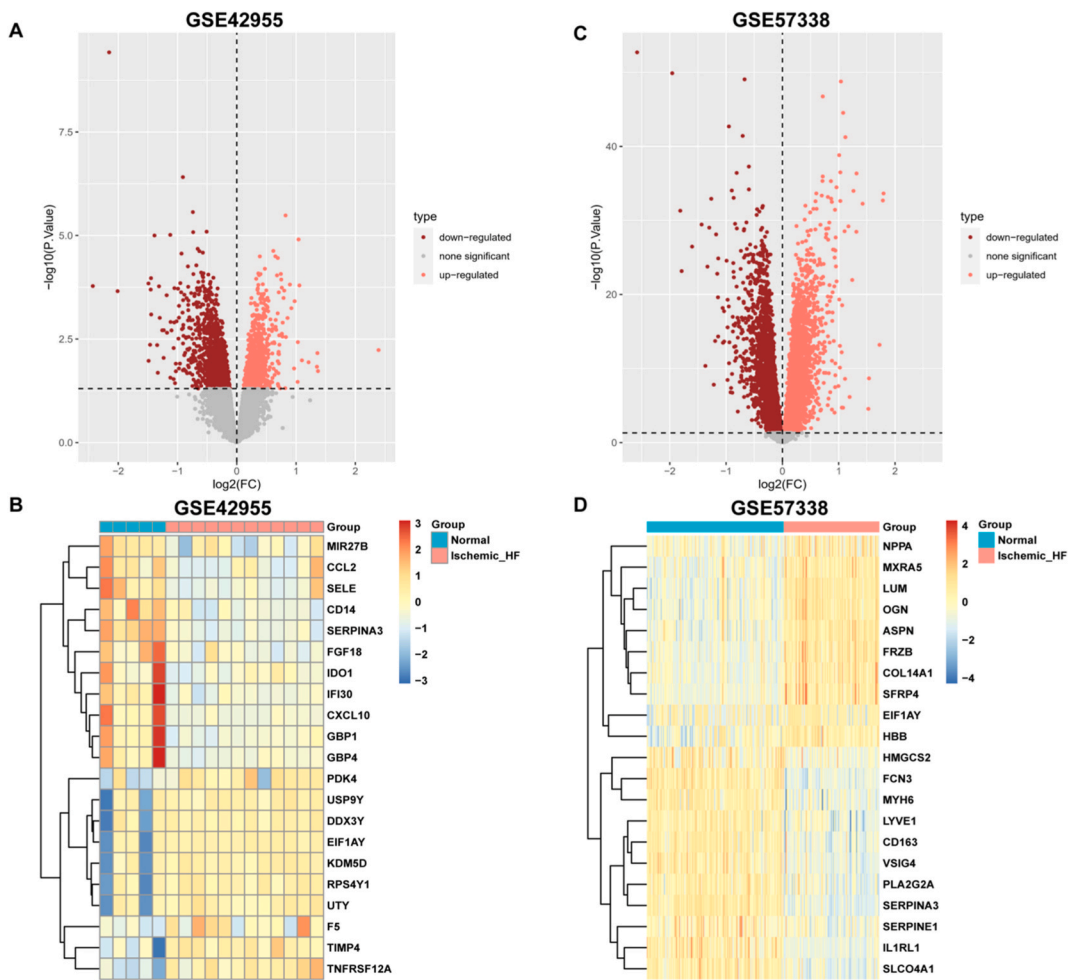


Fig. 1. Identification of differentially expressed genes in IHF datasets. Volcano plots of the differentially expressed genes (DEGs) from GSE42955 (A) and (C) GSE57338 datasets. Dark red dots in the volcano plots represent down-regulated genes, whereas light red points represent up-regulated genes. Heatmaps of the top 10 DEGs from (B) GSE42955 and (D) GSE57338. (For interpretation of the references to color in this figure legend, the reader is referred to the Web version of this article.)

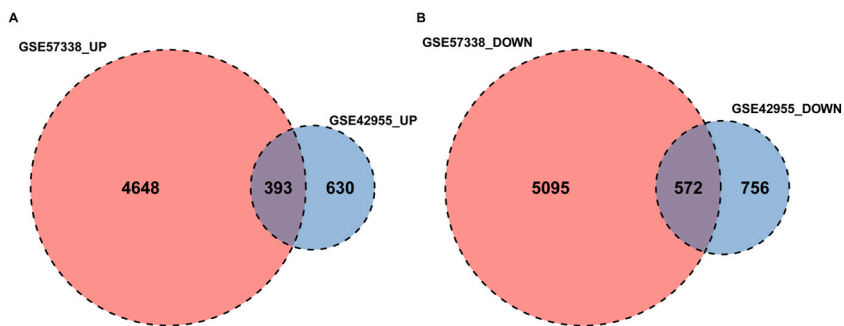


Fig. 2. The Venn plots of DEGs. (A) Up-regulated and (B) down-regulated DEGs from GSE42955 and GSE57338.

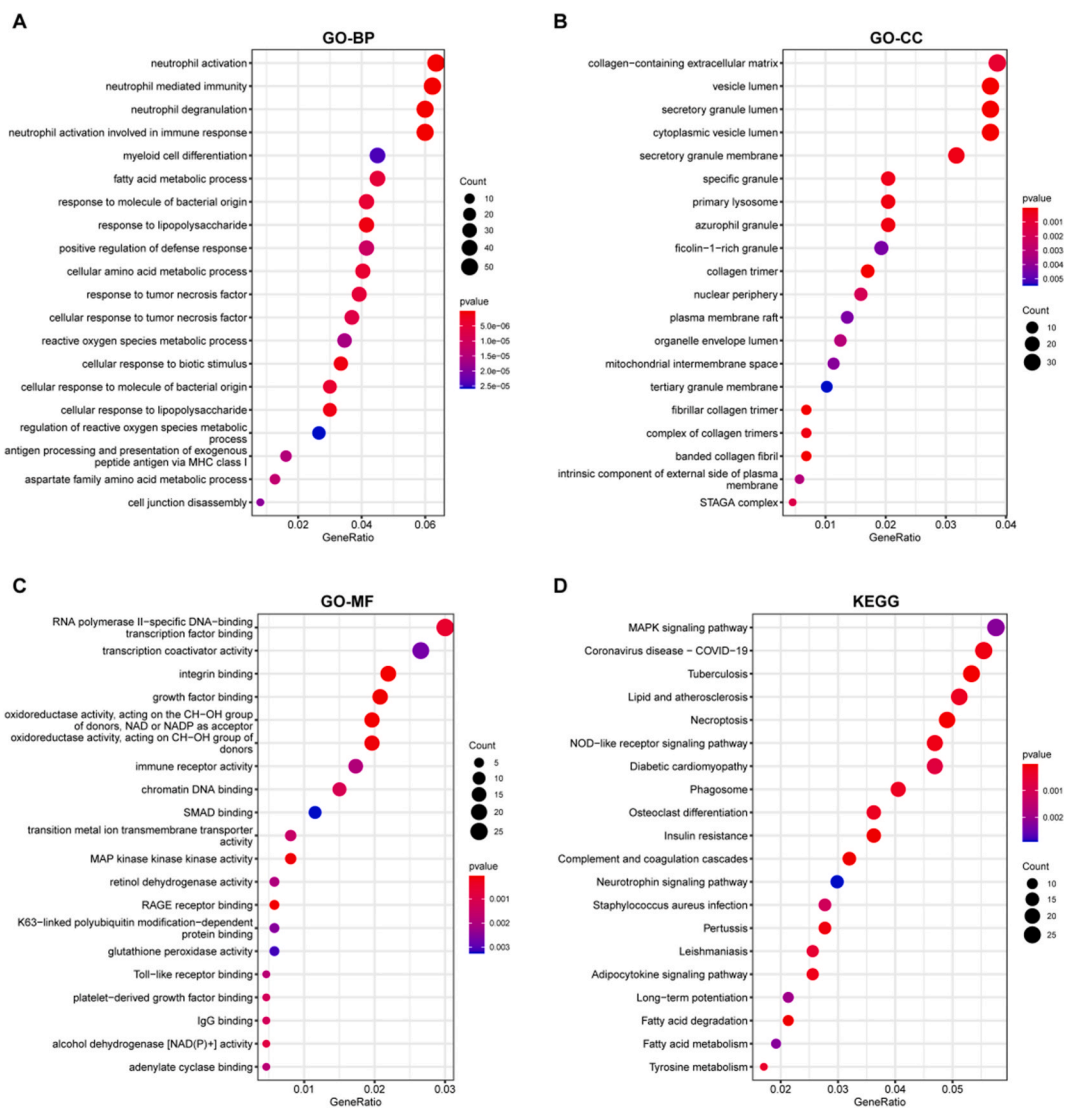


Fig. 3. Enrichment analysis in of DEGs associated with IHF. Gene ontology (GO) enrichment analysis of overlapping DEGs, including (A) BP, (B) CC, and (C) MF. D. KEGG analysis of overlapping DEGs. The top 20 terms are displayed.

tumor types to identify their potential as common targets in HF and cancer.

2. Results

2.1. Identification of differentially expressed genes associated with IHF

The DEGs were screened using GSE42955 and GSE57338 datasets according to the cutoff criterion of a P-value <0.05. The volcano diagram and heat map of the DEGs are shown (Fig. 1A–D). In GSE42955, 1023 genes were up-regulated and 1328 genes were down-regulated. In GSE57338, 5041 genes were up-regulated and 5667 genes were down-regulated. We overlapped the DEGs in GSE42955 and GSE57338 and obtained 393 commonly up-regulated (Fig. 2A) and 572 commonly down-regulated DEGs (Fig. 2B).

2.2. Enrichment analysis of DEGs identified in IHF profiles

We performed GO and KEGG enrichment analyses on the 393 up-regulated and 572 down-regulated DEGs. The GO analysis showed that these DEGs were mainly related to neutrophil activation and myeloid cell differentiation in biological processes (BP) (Fig. 3A); collagen-containing extracellular matrix, secretory granule lumen, and specific granules in cellular components (CC) (Fig. 3B); and transcription factor binding, integrin binding, and growth factor binding in molecular function (MF) (Fig. 3C). For the KEGG results,

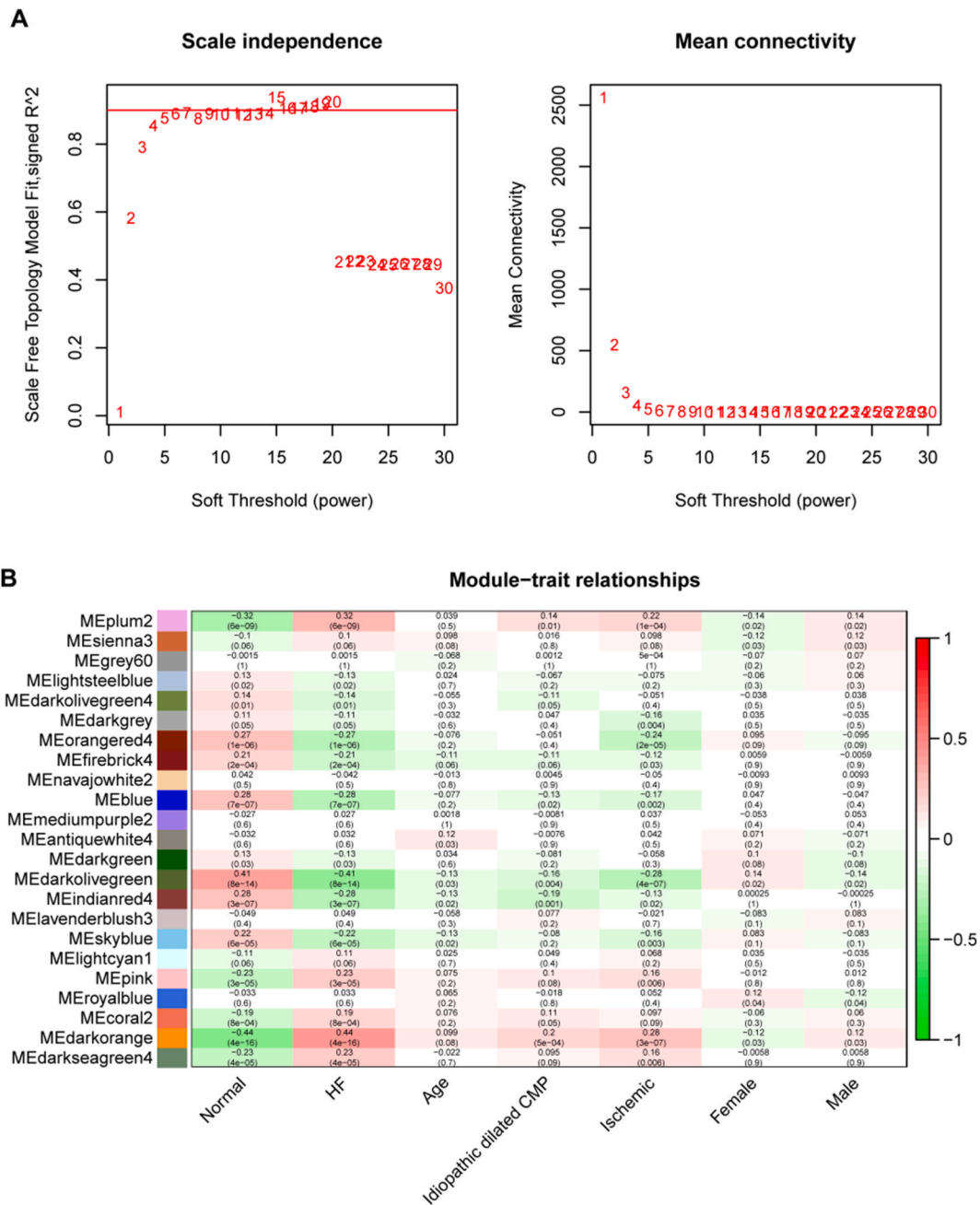


Fig. 4. WGCNA of GSE57338. (A) The selection of best soft threshold. (B) Heatmap of the correlation between the module and clinical features of patients in GSE57338.

the MAPK signaling pathway, coronavirus disease COVID-19, lipid and atherosclerosis, and necroptosis were enriched (Fig. 3D). Together, these results showed pathways involved in HF.

2.3. Construction of a co-expression network and key module identification

Gene co-expression networks were constructed using GSE57338 based on the common DEGs, and a scale-free topology was used to determine the power value. When the power value was 5, the scale-free R^2 approached 0.9 (Fig. 4A). We further screened gene modules associated with HF and selected the MEdarkorange module to conduct the following analysis (Fig. 4B). Next, we intersected the common DEGs and genes from the MEdarkorange module to obtain 85 genes (Fig. 5A). The KEGG analysis indicated that these genes were related to transcriptional misregulation in cancer, ubiquitin-mediated proteolysis, and tumor processes (Fig. 5B and C).

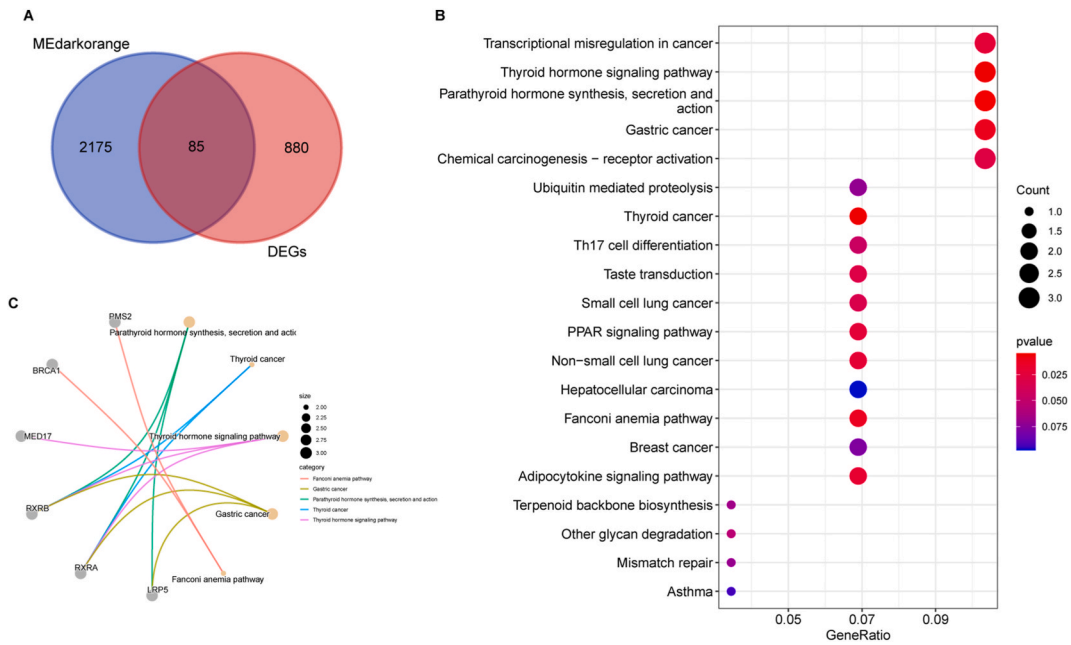


Fig. 5. KEGG enrichment of DEGs from key modules. (A) The intersection between DEGs and genes from the MEDarkorange module. (B) KEGG analysis of overlapping genes. (C). The top five KEGG terms and their correlation with the overlapping genes.

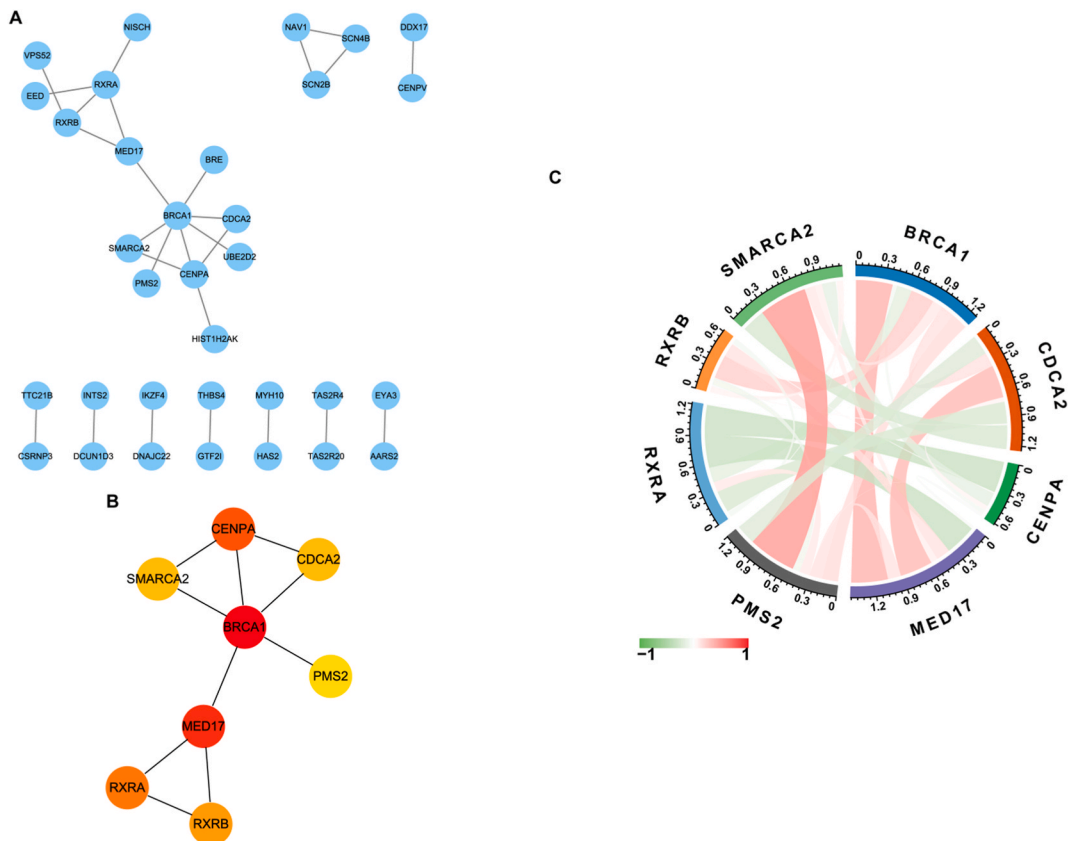


Fig. 6. Identification of hub genes associated with IHF. (A) The protein-protein interaction (PPI) network constructed with the overlapping genes using the STRING database. (B) The top eight hub genes identified by cytoHubba algorithms. (C). The correlation of eight hub genes in GSE57338. The red line represents a positive correlation, green represents a negative correlation, and the deeper the color, the stronger the correlation. (For interpretation of the references to color in this figure legend, the reader is referred to the Web version of this article.)

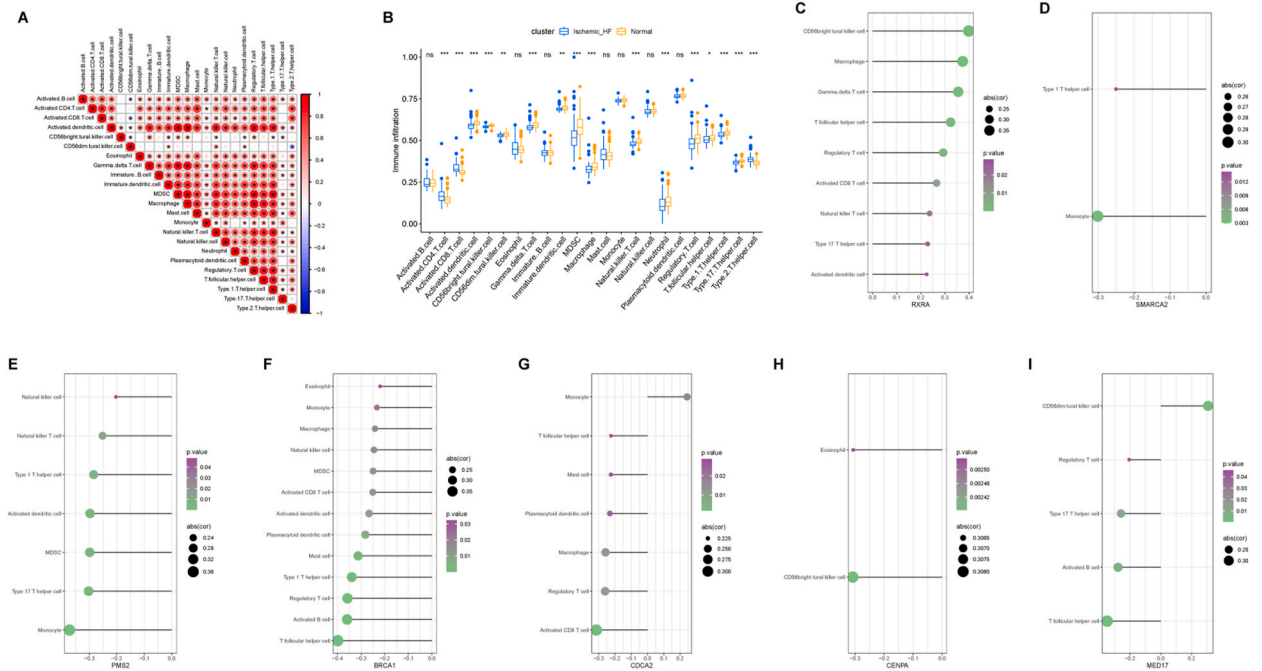


Fig. 7. Correlation analysis of immune cell infiltration and IHF hub gene expression. (A) The correlation between each immune cell. (B) Immune cell infiltration differences between IHF and normal patients. (C) The correlation of immune cell infiltration level with the indicated hub genes. Only significant results ($P < 0.05$) are displayed.

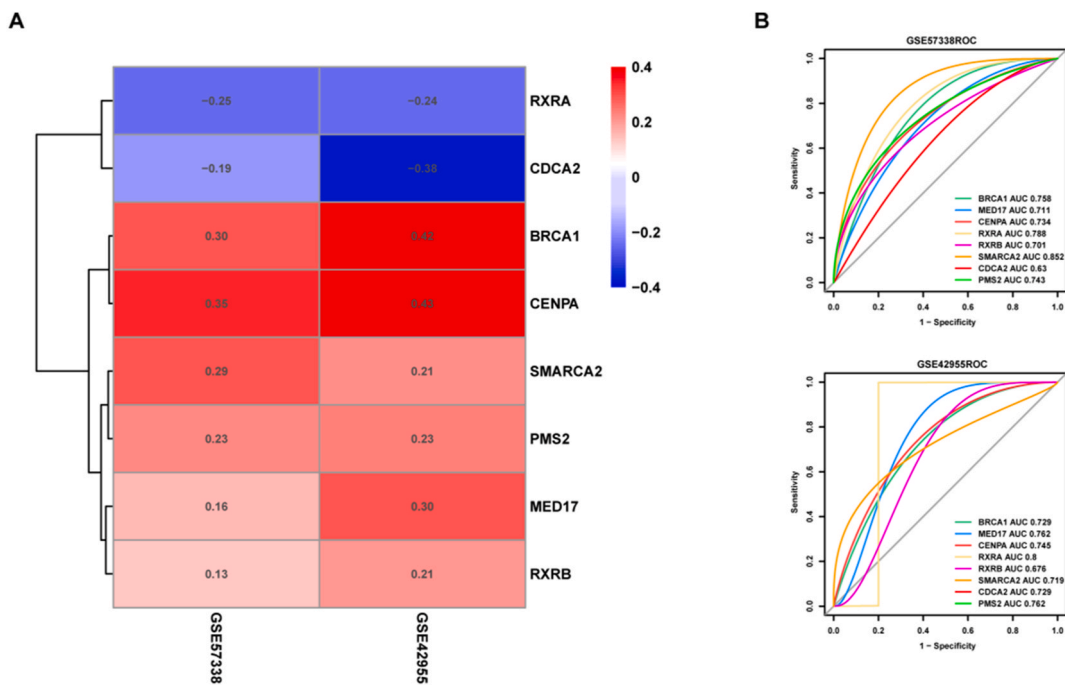


Fig. 8. Exploration of hub genes associated with IHF. (A) Heatmap of the hub genes identified in the GSE57338 and GSE42955 datasets represented as the \log_2 FC values for those genes. (B) Diagnostic efficacy of the eight hub genes for IHF in the GSE57338 and GSE42955 datasets.

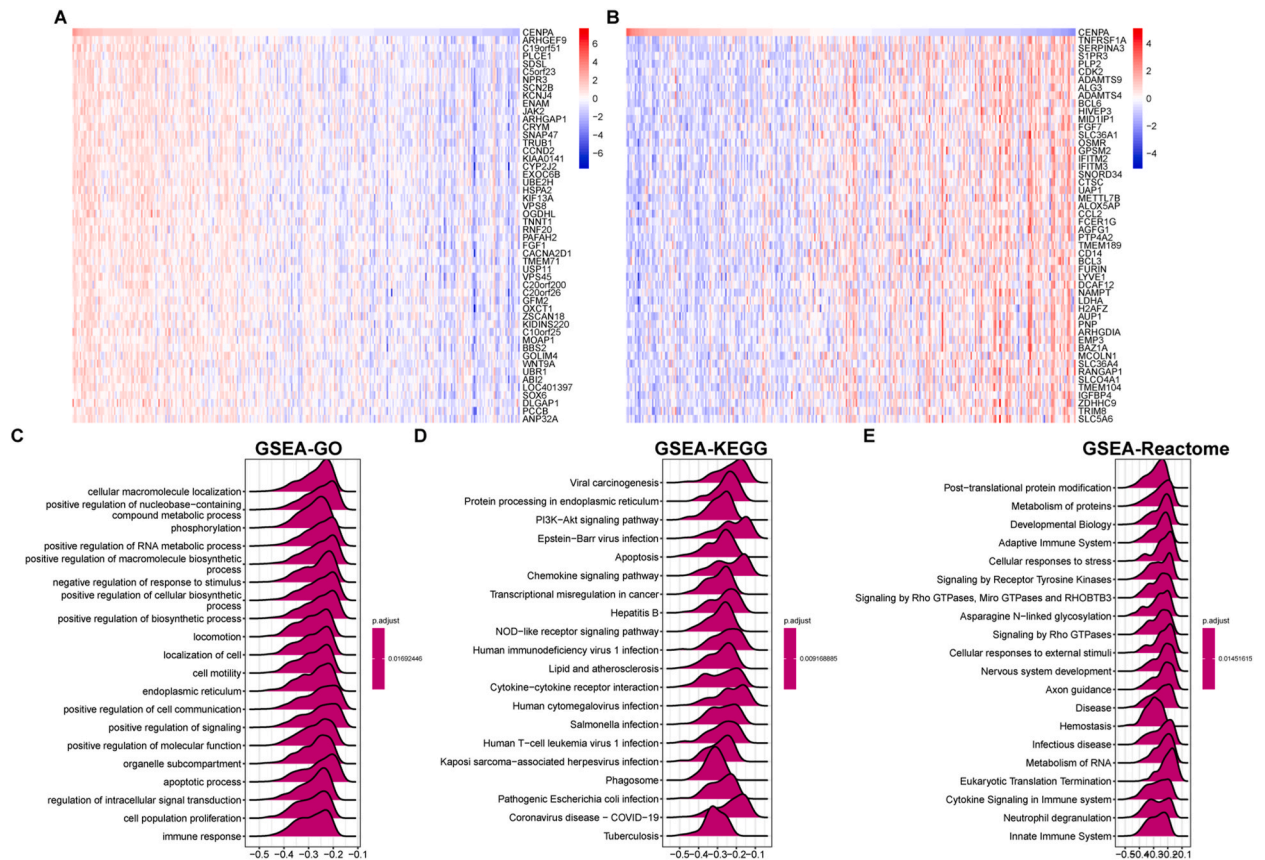


Fig. 9. GSEA of *CENPA*. The correlation analysis of *CENPA* was performed using GSE57338, and the top 50 genes positively (A) and negatively (B) correlated with *CENPA* are displayed. The GSEA of *CENPA* based on GO (C), KEGG (D), and reactome databases (E).

2.4. Protein-protein interaction network construction and identification of hub genes

We imported 85 genes into the STRING online database (<https://string-db.org/>) to create a protein-protein interaction (PPI) network. The PPI network was imported into Cytoscape for visualization (Fig. 6A) and the CytoHubba algorithm was used to identify hub genes. The top eight genes were selected as hub genes for the IHF analysis (Fig. 6B). Correlations between the eight hub genes are shown in Fig. 6C, which shows that *BRCA1* is positively correlated with *MED17* and negatively correlated with *RXRA*.

2.5. Immune infiltration analysis

Immune cell infiltration analysis was performed using GSE57338. Fig. 7A shows the correlation with immune cell infiltration. Most immune cells were differentially infiltrated between IHF and normal samples (Fig. 7B). For example, macrophage and natural killer T cell infiltration were lower in the IHF group than control group. Fig. 7C–I shows the correlation between the hub genes and immune cell infiltration (P-value <0.05).

2.6. Hub gene analysis

The top eight hub genes (*BRCA1*, *MED17*, *CENPA*, *RXRA*, *RXRB*, *SMARCA2*, *CDCA2*, and *PMS2*) we identified using the CytoHubba algorithm were further analyzed. The log₂ (fold-change) value of each gene in the two datasets is shown in Fig. 8A. Moreover, we analyzed the diagnostic efficacy of the eight hub genes for IHF in both the GSE42955 and GSE57338 datasets, which showed the great performance in distinguishing diseases tissues from normal tissues (Fig. 8B). We explored the functions of these genes in IHF using *CENPA* and *BRCA1*. Through correlation analysis, we displayed the expression of the top 50 genes positively and negatively correlated with *CENPA* (Fig. 9A and B) and *BRCA1* (Supplemental Fig. 1A and B). GSEA was also performed on the correlation analysis results, which indicated that *CENPA* was associated with cellular macromolecule localization in GSEA-GO enrichment (Fig. 9C); the viral carcinogenesis and PI3K–Akt signaling pathway in GSEA-KEGG enrichment (Fig. 9D); and post-translational protein modification, metabolism of proteins, adaptive immune system, and cellular responses to stress in GSEA-reactome enrichment (Fig. 9E). *BRCA1* was associated with mitochondrion in GSEA-GO enrichment (Supplemental Figure 1C); the valine, leucine and isoleucine degradation and

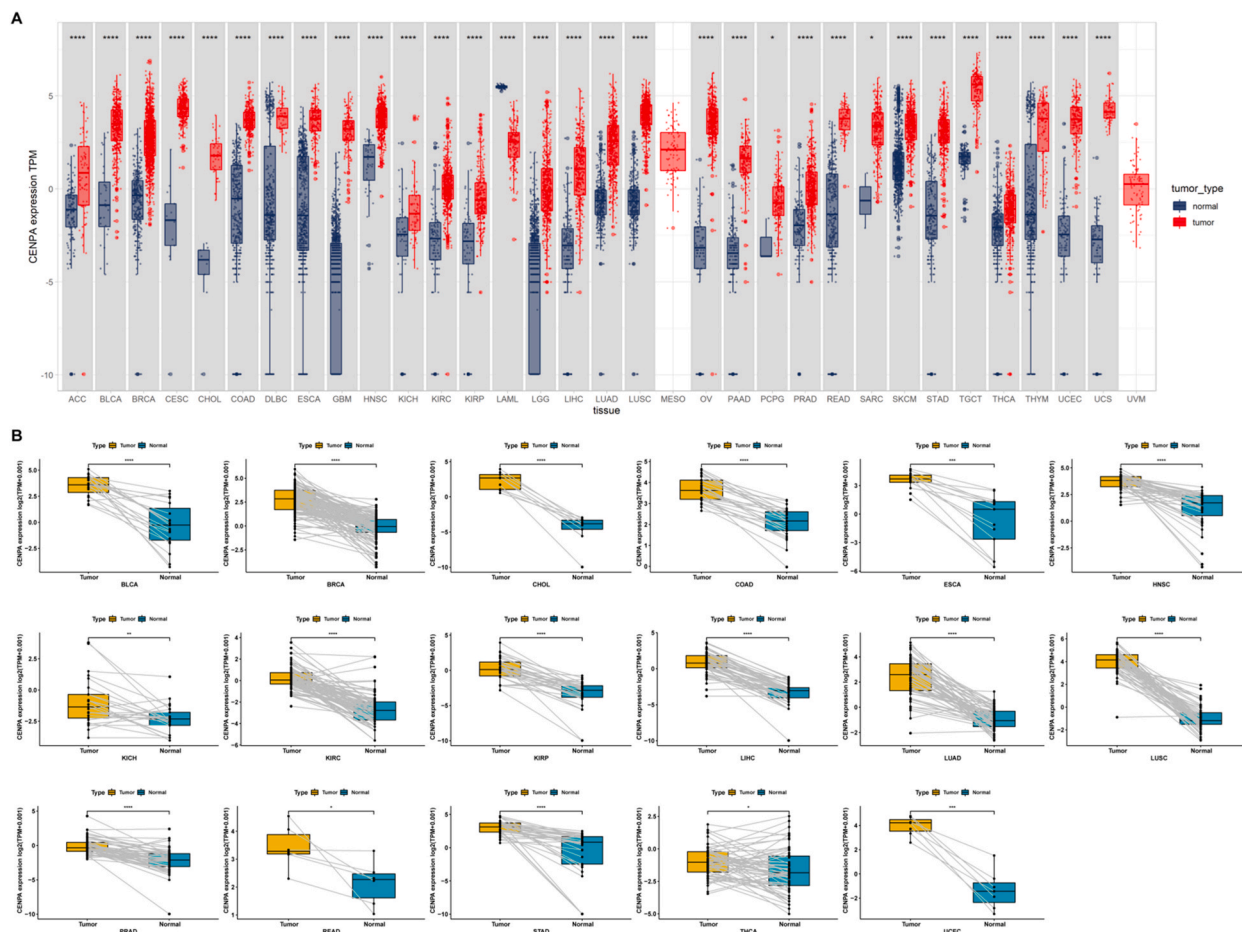


Fig. 10. Pan-cancer CENPA expression analysis. (A) Pan-cancer differential expression of *CENPA* between tumor tissues from TCGA and normal tissues from TCGA and GTEx databases. (B) Pan-cancer differential expression of *CENPA* between tumor tissues and paired adjacent normal tissues.

hippo signaling pathway in GSEA-KEGG enrichment (Supplemental Figure 1D); the citric acid cycle (TCA) and respiratory electron transport, protein localization, mitochondrial translation in GSEA-Reactome enrichment (Supplemental Figure 1E).

2.7. Pan-cancer analysis of hub genes

Next, we selected *CENPA* and *BRCA1* for pan-cancer analysis. We found that *CENPA* and *BRCA1* were highly expressed in tumor tissues from the TCGA database compared to normal tissues from TCGA and GTEx databases (Fig. 10A and Supplemental Figure 2A). When we analyzed *CENPA* and *BRCA1* expression from the TCGA database, we found that *CENPA* and *BRCA1* were overexpressed in tumor tissues compared to matched para-cancerous tissues in most tumor types (Fig. 10B and Supplemental Figure 2B). For *CENPA*, we evaluated the relationship between *CENPA* expression and patient prognosis in pan-cancer using survival metrics, including overall survival (OS), disease-specific survival (DSS), disease-free interval (DFI), and progression-free interval (PFI). Cox regression analysis of 33 tumors showed that high *CENPA* expression was significantly associated with a worse prognosis for multiple cancers, especially KIRP, ACC, LIHC, and PAAD, for all survival indices (Fig. 11A–D and Supplemental Fig. 3A–D).

To explore the biological significance of *CENPA* and *BRCA1* expression in different tumor tissues, we analyzed the correlation between their expression and 50 HALLMARK pathways. We found that both *CENPA* and *BRCA1* were most strongly associated with cell cycle-related pathways such as the G2M checkpoint and E2F target pathways (Fig. 12A and B). We also analyzed the correlation between *CENPA*, *BRCA1*, and immune cell infiltration in pan-cancer samples. The results indicated that patients with a higher expression of these genes had lower infiltration levels (Fig. 13A and B).

Finally, we analyzed the relationship between *CENPA*, *BRCA1*, and drug resistance to provide suitable medications selections for patients (Supplemental Table 1). Among the 192 anti-tumor drugs in the GDSC database, *CENPA* expression was positively correlated with the IC50 of 13 drugs, including BMS-754807, Trametinib, SCH772984, Selumetinib, ERK_6604, and SB216763 (Fig. 14). These results suggested that *CENPA* and *BRCA1* have clinical potential as drug targets in multiple cancers.

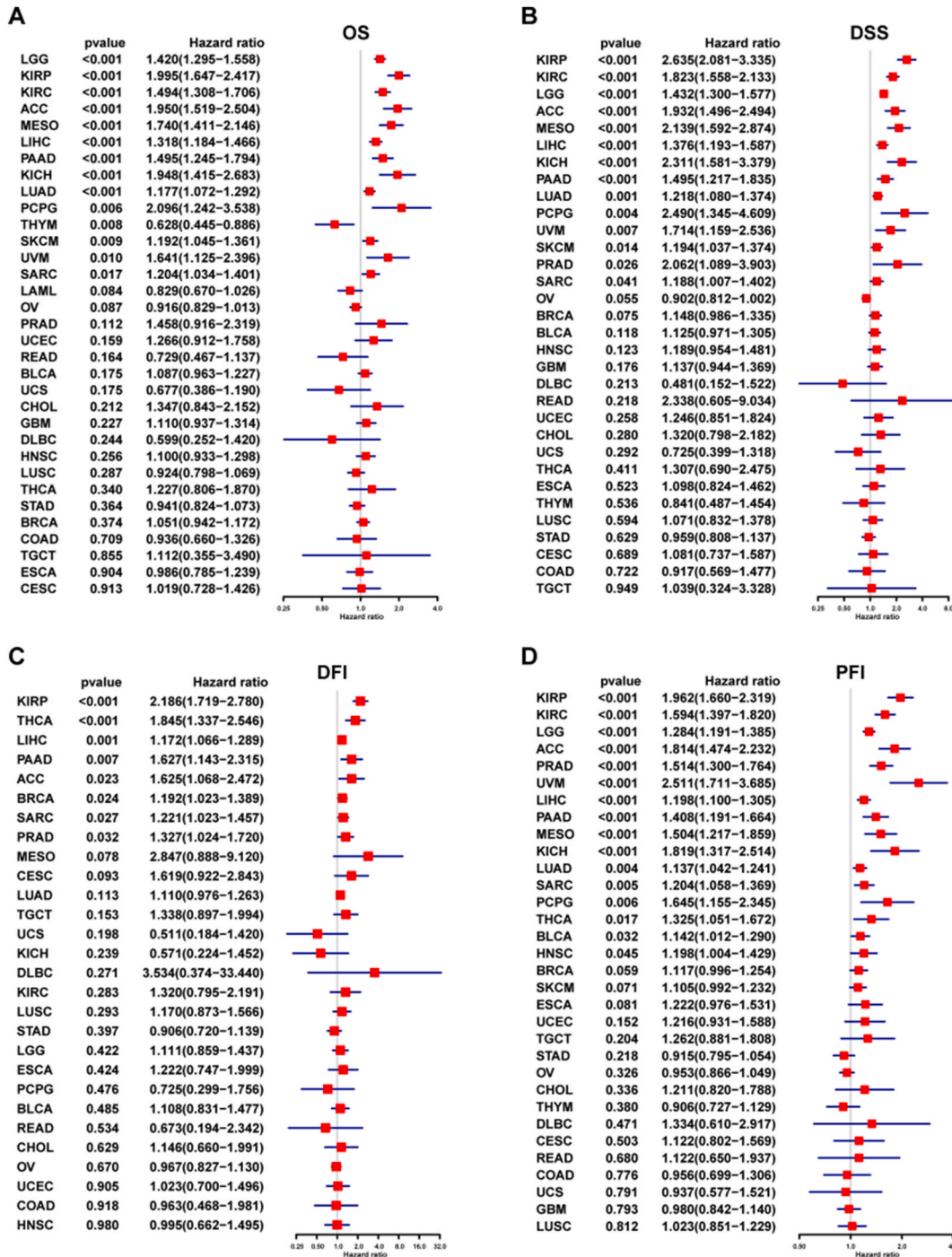


Fig. 11. Univariate regression analysis of *CENPA* expression in pan-cancer. Forest map showing the univariate Cox regression analysis results of *CENPA* from the TCGA pan-cancer data, including (A) OS, (B) DSS, (C) DFI, and (D) PFI.

3. Discussion

Heart failure (HF) and cancer remains the leading causes of mortality and poses major burdens on healthcare worldwide [16-18]. Over the years the bidirectional link between HF and cancer has been gradually uncovered, but the mechanism on the reciprocal effect of both diseases and how HF increases the risk of cancer is incompletely understood [9,10,19]. Therefore, it is increasingly important to identify common targets for HF and cancer. We used integrated bioinformatics analyses, including differential expression analysis

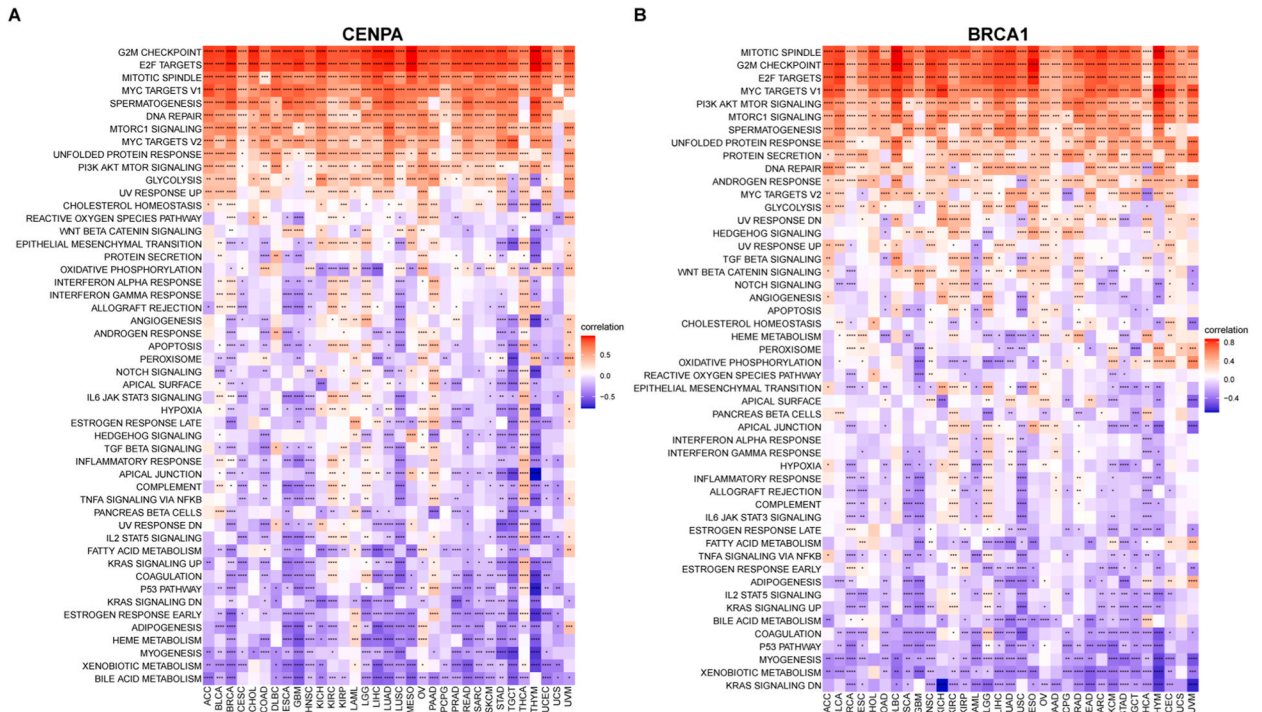


Fig. 12. GSVA of *CENPA* and *BRCA1*. The GSVA results of (A) *CENPA* and (B) *BRCA1* based on 50 HALLMARK pathways in pan-cancer. * $P < 0.05$, ** $P < 0.01$, *** $P < 0.001$, **** $P < 0.0001$.

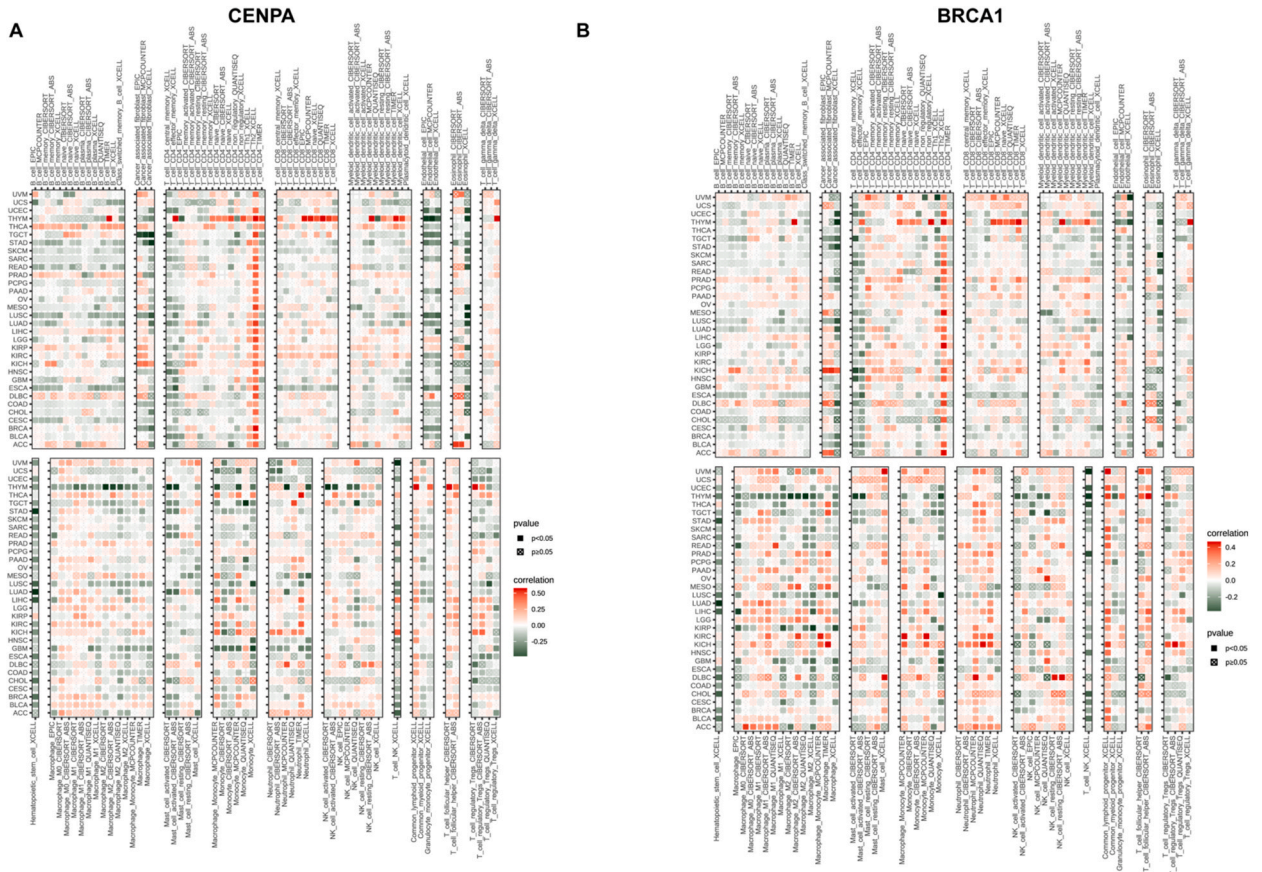


Fig. 13. Immune infiltration analysis. (A–B) The relationship between gene expression and infiltration levels of different types of immune cells in pan-cancer.

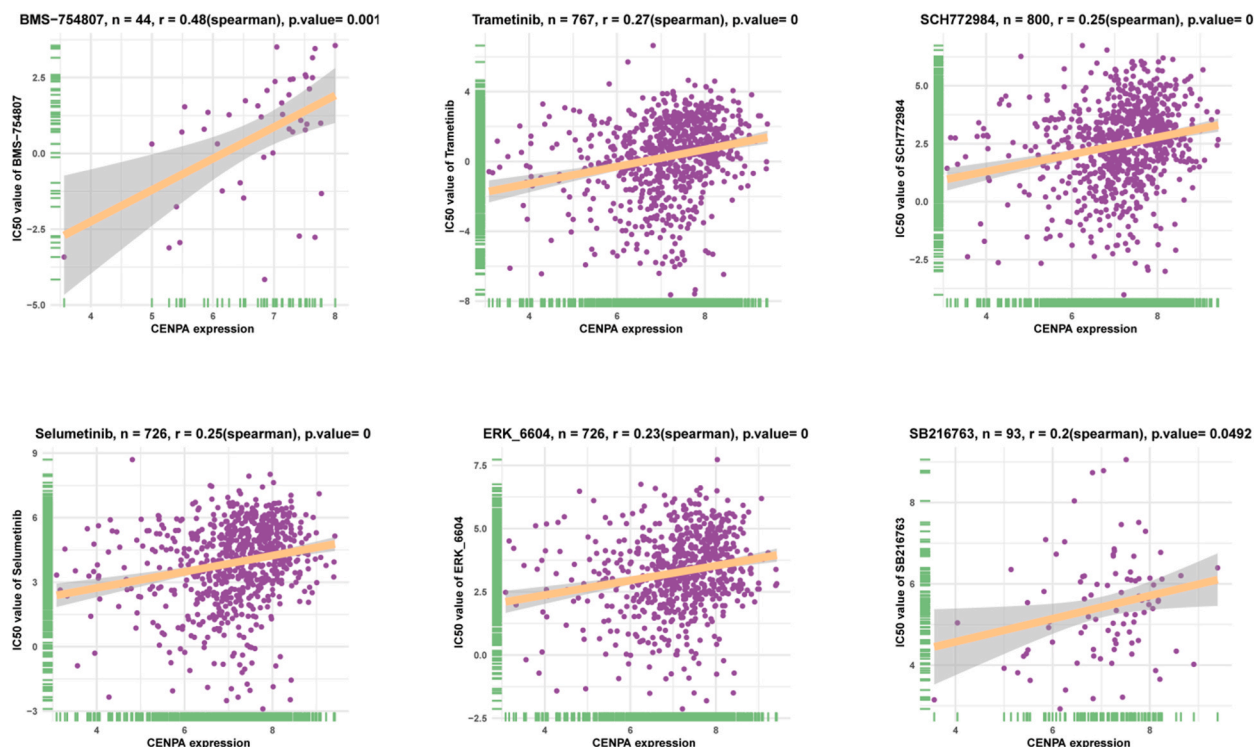


Fig. 14. *CENPA* expression and drug resistance are correlated in pan-cancer. Correlation between *CENPA* expression and the IC50 values of anticancer drugs. $P = 0$ indicates $P < 0.0001$.

and WGCNA, to identify hub genes related to IHF. These genes were subjected to GO enrichment analysis, which revealed that they were primarily enriched in transcriptional misregulation in cancer, ubiquitin mediated proteolysis, and tumor processes, indicating that these genes may be associated with tumor progression. Among the hub genes associated with IHF, *BRCA1*, *MED17*, *CENPA*, *RXRβ*, *SMARCA2*, and *PMS2* were up-regulated in patients with IHF, whereas *RXRA* and *CDCA2* were down-regulated in IHF patients.

Previous studies revealed that multiple immune cells infiltrations and activations, including macrophages, neutrophils, B cells, T cells and regulatory T cells, played an important role in the pathological processes of HF and myocardial remodeling [20–22], and cancer [23–25]. *CALU*, *PALLD*, *FOS*, *DUSP1* have been identified as potential biomarkers of immune cell infiltration in HF [26,27]. Disorders of the immune system and abnormal activation of immune signaling pathway could cause the co-occurrence of HF and lung cancer [28]. Although the augmented immune response will lead to immune-related HF [29], transient chimeric antigen receptor (CAR) T cells *in vivo* reduced myocardial fibrosis and restored cardiac function after injury [30]. In this study, we found that most immune cells were differentially infiltrated in IHF and normal samples, of which macrophage infiltration was low in the IHF group and *BRCA1* was negatively correlated with macrophage infiltration. These results are partly consistent with previous studies [21,31].

HF and cancer accompany each other given the large overlap in risk factors [7]. Indeed, it has been reported that HF and cancer often coincide and there is evidence of a direct effect between both diseases [3,7,14,19,32,33]. Our study found that *CENPA* and *BRCA1* were biomarkers of HF and cancer, and strongly associated with cell division and cycle-related pathways such as the G2M checkpoint and E2F target pathways. The centromere-specific histone H3 variant *CENPA* and the tumor suppressor *BRCA1* have been reported the key role in preserving centromeric integrity during cell division or DNA damage [34,35]. *BRCA1*-deficient cells showed impaired localization of *CENPA*, leading to impaired chromosome inheritance and genome instability [34]. *CENPA* overexpression promoted genome instability in human cells [36]. Furthermore, these genes have been reported to be therapeutic targets in many tumor types, including breast [37–39], liver [40,41], and ovarian [42,43] cancers. Thus, we assessed the roles of *BRCA1* and *CENPA* in pan-cancer to explore them as common targets of IHF and cancer among the hub genes. We found that *CENPA* and *BRCA1* were ubiquitously expressed in tumors and correlated with poor prognosis in patients with cancer. We believe that drugs targeting *CENPA* or *BRCA1* might be effective in patients with HF and cancer.

To conclude, our study identified that *CENPA* and *BRCA1* were potential therapeutic targets associated with immune cell infiltration for both HF and cancer, which provided new perspectives for expanding our understanding of pathophysiological interaction mechanisms of HF and cancer. Meanwhile, the conclusion only originated from the bioinformatic analysis on shared datasets with limited sample size. The heterogeneity of patients or heart samples, RNA sequencing platforms and methods may increase the risk of bias. Further validation of *CENPA* and *BRCA1* in larger, independent cohorts or investigation on the potential mechanism in laboratory, as well as explorations on simple and feasible methods for detections of *CENPA* and *BRCA1* in clinical practice will be suggested for future research.

4. Materials and methods

4.1. Acquisition of datasets

Gene expression profiles of GSE42955 and GSE57338 were acquired from human samples and downloaded from the Gene Expression Omnibus (GEO) database (<http://www.ncbi.nih.gov/geo/>). GSE42955 includes transmural heart samples near the apex of the left ventricle from 12 ischemic cardiomyopathy patients, 12 dilated cardiomyopathy patients and 5 normal controls. Meanwhile we downloaded 95 ischemic cardiomyopathy and 136 normal tissue samples of the left ventricle from the GSE57338 dataset, which contained a total of 313 individuals with/without heart failure. The expression of *CENPA* and *BRCA1* in 31 normal tissues was obtained from the GTEx portal and was compared between 33 cancer and normal tissues by combining data from TCGA with those from GTEx. The combined TCGA and GTEx data were downloaded from the UCSC Xena database (<https://xenabrowser.net/datapages/>).

4.2. Identifying key co-expression modules using weighted gene co-expression network analysis

We used the R package “WGCNA” to construct a gene co-expression network from the GSE57338 dataset GEO series. We analyzed the correlation between the modules and clinical features. The modules closely related to HF were used for subsequent analyses.

4.3. Identification of differentially expressed genes and selection of potential target genes

To identify differentially expressed genes (DEGs) between IHF and normal controls, we performed DEG analysis based on the gene expression profiles of GSE42955 and GSE57338 using the ‘limma’ package. The cut-off value was set to a P-value <0.05. The overlapping genes were selected for subsequent analyses.

4.4. Enrichment analysis

We performed Gene Ontology (GO) and Kyoto Encyclopedia of Genes and Genomes (KEGG) enrichment analysis using the “clusterProfiler” R package to evaluate the biological significance of selected genes. We downloaded 50 HALLMARK pathways from the MsigDB database (<http://www.gsea-msigdb.org/gsea/msigdb/index.jsp>) and used the “GSVA” package to score the pathways and calculate their correlation with gene expression in pan-cancer.

4.5. Construction of protein-protein networks and screening for hub genes

For partially overlapping genes, we created protein-protein interaction (PPI) networks using the STRING database (<https://string-db.org>). The PPI network was visualized in Cytoscape [44]. The top eight hub genes were identified with the plug-in ‘cytoHubba’ and used for the subsequent analysis.

4.6. Tumor microenvironment analysis

From the TIMER2 (<http://timer.comp-genomics.org/>) database, we downloaded pan-cancer immune cell infiltration data. The correlation between gene expression and immune cells was calculated.

4.7. Drug sensitivity analysis

We downloaded the half-maximal inhibitory concentration (IC50) and gene expression data of tumor cells from the GDSC (<https://www.cancerrxgene.org/>) database, analyzed the relationship between gene expression and drug IC50, and plotted the correlation between *CENPA* expression for each drug and IC50.

Funding statement

This work was supported by Chengdu High-level Key Clinical Specialty Construction Project 2020, Fundamental Research Funds for the Central Universities (Grant No. 2682022ZTPY029, 2682021ZTPY026), Science and Technology Research Project of Sichuan Provincial Traditional Chinese Medicine Administration (Grant No. 2023MS288), Technology Innovation Research Project of Chengdu Science and Technology Bureau (Grant No. 2019-YF05-00523-SN).

CRedit authorship contribution statement

Jian Wang: Writing – original draft, Methodology. **Lin Cai:** Supervision, Methodology. **Gang Huang:** Writing – original draft, Funding acquisition, Data curation. **Chunbin Wang:** Methodology, Funding acquisition, Data curation. **Zhen Zhang:** Writing – review & editing, Supervision, Conceptualization. **Junbo Xu:** Writing – review & editing, Supervision, Funding acquisition, Conceptualization.

Declaration of competing interest

The authors declare that they have no known competing financial interests or personal relationships that could have appeared to influence the work reported in this paper.

Acknowledgements

We thank Dr. Chengdong Liu from Southern Medical University for his technical support on bioinformatics analysis, and the TCGA and GEO platforms for providing public datasets and their contributors for updating the datasets. Users can download the relevant data for free for their research and publishing their experimental findings. Ethical approval was obtained from all patients included in the database. Our study was based on open-source data; therefore, there were no ethical issues or conflicts of interest.

Appendix A. Supplementary data

Supplementary data to this article can be found online at <https://doi.org/10.1016/j.heliyon.2024.e28786>.

References

- [1] P. Thavandiranathan, M.T. Nolan, An emerging epidemic: cancer and heart failure, *Clin. Sci.* 131 (2) (2017) 113–121.
- [2] G. Savarese, et al., Global burden of heart failure: a comprehensive and updated review of epidemiology, *Cardiovasc. Res.* 118 (17) (2023) 3272–3287.
- [3] T. Hasin, et al., Patients with heart failure have an increased risk of incident cancer, *J. Am. Coll. Cardiol.* 62 (10) (2013) 881–886.
- [4] T. Hasin, et al., Heart failure after myocardial infarction is associated with increased risk of cancer, *J. Am. Coll. Cardiol.* 68 (3) (2016) 265–271.
- [5] A. Banke, et al., Incidence of cancer in patients with chronic heart failure: a long-term follow-up study, *Eur. J. Heart Fail.* 18 (3) (2016) 260–266.
- [6] E. Bertero, et al., Cancer incidence and mortality according to pre-existing heart failure in a community-based cohort, *JACC. CardioOncology* 4 (1) (2022) 98–109.
- [7] W.C. Meijers, R.A. de Boer, Common risk factors for heart failure and cancer, *Cardiovasc. Res.* 115 (5) (2019) 844–853.
- [8] R.A. de Boer, et al., Common mechanistic pathways in cancer and heart failure. A scientific roadmap on behalf of the translational research committee of the heart failure association (HFA) of the European society of cardiology (ESC), *Eur. J. Heart Fail.* 22 (12) (2020) 2272–2289.
- [9] R.A. de Boer, et al., Cancer and heart disease: associations and relations, *Eur. J. Heart Fail.* 21 (12) (2019) 1515–1525.
- [10] M. Chianca, et al., Bidirectional relationship between cancer and heart failure: insights on circulating biomarkers, *Frontiers in Cardiovascular Medicine* 9 (2022) 936654.
- [11] A.R. Lyon, et al., ESC guidelines on cardio-oncology developed in collaboration with the European hematology association (EHA), the European society for therapeutic Radiology and Oncology (ESTRO) and the International Cardio-Oncology Society (IC-OS), *Eur. Heart J.* 43 (41) (2022) 4229–4361, 2022.
- [12] R.A. de Boer, et al., Cancer and heart disease: associations and relations, *Eur. J. Heart Fail.* 21 (12) (2019) 1515–1525.
- [13] M.S. Anker, et al., Advanced cancer is also a heart failure syndrome: a hypothesis, *Journal of Cachexia, Sarcopenia and Muscle* 12 (3) (2021) 533–537.
- [14] W.C. Meijers, et al., Heart failure stimulates tumor growth by circulating factors, *Circulation* 138 (7) (2018) 678–691.
- [15] L. Awwad, A. Aronheim, Cardiac dysfunction promotes cancer progression via multiple secreted factors, *Cancer Res.* 82 (9) (2022) 1753–1761.
- [16] P. Severino, et al., Ischemic heart disease pathophysiology paradigms overview: from plaque activation to microvascular dysfunction, *Int. J. Mol. Sci.* 21 (21) (2020).
- [17] J.-H. Chen, et al., Identification of MYH6 as the potential gene for human ischaemic cardiomyopathy, *J. Cell Mol. Med.* 25 (22) (2021) 10736–10746.
- [18] R.L. Siegel, A.N. Giaquinto, A. Jemal, Cancer statistics, *CA A Cancer J. Clin.* 74 (1) (2024) 12–49, 2024.
- [19] R.N. Kitsis, J.A. Riquelme, S. Lavandero, Heart disease and cancer: are the two killers colluding? *Circulation* 138 (7) (2018) 692–695.
- [20] E. Martini, et al., Single-cell sequencing of mouse heart immune infiltrate in pressure overload-driven heart failure reveals extent of immune activation, *Circulation* 140 (25) (2019) 2089–2107.
- [21] N.R. Wong, et al., Resident cardiac macrophages mediate adaptive myocardial remodeling, *Immunity* 54 (9) (2021).
- [22] F.K. Swirski, M. Nahrendorf, Cardioimmunology: the immune system in cardiac homeostasis and disease, *Nat. Rev. Immunol.* 18 (12) (2018) 733–744.
- [23] R.D. Schreiber, L.J. Old, M.J. Smyth, Cancer immunoeediting: integrating immunity's roles in cancer suppression and promotion, *Science* 331 (6024) (2011) 1565–1570. New York, N.Y.
- [24] T.F. Gajewski, H. Schreiber, Y.-X. Fu, Innate and adaptive immune cells in the tumor microenvironment, *Nat. Immunol.* 14 (10) (2013) 1014–1022.
- [25] R. Rui, L. Zhou, S. He, Cancer immunotherapies: advances and bottlenecks, *Front. Immunol.* 14 (2023) 1212476.
- [26] X. Liu, et al., Identification of CALU and PALLD as potential biomarkers associated with immune infiltration in heart failure, *Frontiers In Cardiovascular Medicine* 8 (2021) 774755.
- [27] W. Liu, et al., Identification of biomarkers and immune infiltration in acute myocardial infarction and heart failure by integrated analysis, *Biosci. Rep.* 43 (7) (2023).
- [28] X. Wang, et al., Bioinformatics analysis of the genes associated with co-occurrence of heart failure and lung cancer, *Exp. Biol. Med.* 248 (10) (2023) 843–857.
- [29] J.-R. Hu, et al., Cardiovascular toxicities associated with immune checkpoint inhibitors, *Cardiovasc. Res.* 115 (5) (2019) 854–868.
- [30] J.G. Rurik, et al., CAR T cells produced in vivo to treat cardiac injury, *Science (New York, N.Y.)* 375 (6576) (2022) 91–96.
- [31] N. Zhang, et al., CXCR4-dependent macrophage-to-fibroblast signaling contributes to cardiac diastolic dysfunction in heart failure with preserved ejection fraction, *Int. J. Biol. Sci.* 18 (3) (2022) 1271–1287.
- [32] E. Bertero, et al., Linking heart failure to cancer: background evidence and research perspectives, *Circulation* 138 (7) (2018) 735–742.
- [33] R.J. Koene, et al., Shared risk factors in cardiovascular disease and cancer, *Circulation* 133 (11) (2016) 1104–1114.
- [34] C. Racca, et al., BRCA1 prevents R-loop-associated centromeric instability, *Cell Death Dis.* 12 (10) (2021) 896.
- [35] D. Yilmaz, et al., Activation of homologous recombination in G1 preserves centromeric integrity, *Nature* 600 (7890) (2021) 748–753.
- [36] A. Amato, et al., CENPA overexpression promotes genome instability in pRb-depleted human cells, *Mol. Cancer* 8 (2009) 119.
- [37] K. Yoshida, Y. Miki, Role of BRCA1 and BRCA2 as regulators of DNA repair, transcription, and cell cycle in response to DNA damage, *Cancer Sci.* 95 (11) (2004) 866–871.
- [38] A.S. Algebaly, R.S. Suliman, W.S. Al-Qahtani, Comprehensive study for BRCA1 and BRCA2 entire coding regions in breast cancer, in: *Clinical & Translational Oncology* : Official Publication of the Federation of Spanish Oncology Societies and of the, National Cancer Institute of Mexico, 2021, pp. 74–81, 23(1).
- [39] A.B. Rajput, et al., Immunohistochemical assessment of expression of centromere protein-A (CENPA) in human invasive breast cancer, *Cancers* 3 (4) (2011) 4212–4227.

- [40] J. Zhao, et al., Olaparib and enzalutamide synergistically suppress HCC progression via the AR-mediated miR-146a-5p/BRCA1 signaling, in: *FASEB Journal*, Official Publication of the Federation of American Societies For Experimental Biology, 2020, pp. 5877–5891, 34(4).
- [41] J. Long, et al., A four-gene-based prognostic model predicts overall survival in patients with hepatocellular carcinoma, *J. Cell Mol. Med.* 22 (12) (2018) 5928–5938.
- [42] P.J. O'Donovan, D.M. Livingston, BRCA1 and BRCA2: breast/ovarian cancer susceptibility gene products and participants in DNA double-strand break repair, *Carcinogenesis* 31 (6) (2010) 961–967.
- [43] J. Han, et al., CENPA is one of the potential key genes associated with the proliferation and prognosis of ovarian cancer based on integrated bioinformatics analysis and regulated by MYBL2, *Transl. Cancer Res.* 10 (9) (2021) 4076–4086.
- [44] P. Shannon, et al., Cytoscape: a software environment for integrated models of biomolecular interaction networks, *Genome Res.* 13 (11) (2003) 2498–2504.